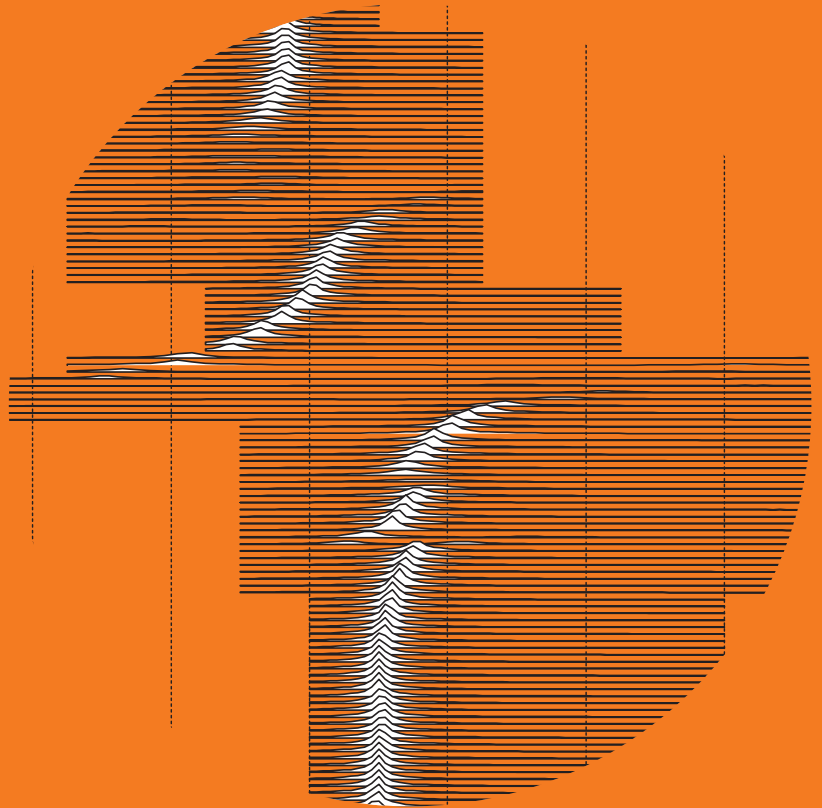


O.V. Lounasmaa Laboratory

Experimental studies on dilute helium mixtures at low temperatures

Anssi Salmela



Experimental studies on dilute helium mixtures at low temperatures

Anssi Salmela

Doctoral dissertation for the degree of Doctor of Science in Technology to be presented with due permission of the School of Science for public examination and debate in Auditorium N at the Aalto University School of Science (Espoo, Finland) on the 27th of April 2012 at 12 noon.

Aalto University
Aalto University School of Science
O.V. Lounasmaa Laboratory
YKI group

Supervisor

Professor Matti Kaivola

Instructor

Docent Juha Tuoriniemi

Preliminary examiners

Docent Sergey Vasiliev, University of Turku, Finland

Doctor Jan Nyeki, Royal Holloway, University of London, United Kingdom

Opponent

Professor Ladislav Skrbek, Charles University, Czech Republic

Aalto University publication series

DOCTORAL DISSERTATIONS 43/2012

© Anssi Salmela

ISBN 978-952-60-4582-5 (printed)

ISBN 978-952-60-4583-2 (pdf)

ISSN-L 1799-4934

ISSN 1799-4934 (printed)

ISSN 1799-4942 (pdf)

Unigrafia Oy

Helsinki 2012

Finland

The dissertation can be read at <http://lib.tkk.fi/Diss/>



Author

Anssi Salmela

Name of the doctoral dissertation

Experimental studies on dilute helium mixtures at low temperatures

Publisher Aalto University School of Science

Unit O.V. Lounasmaa Laboratory

Series Aalto University publication series DOCTORAL DISSERTATIONS 43/2012

Field of research Experimental condensed matter physics

Manuscript submitted 24 January 2012 **Manuscript revised** 16 March 2012

Date of the defence 27 April 2012 **Language** English

Monograph **Article dissertation (summary + original articles)**

Abstract

When cooled to almost zero temperature, helium offers a very versatile subject for the experimental study of quantum matter. The two stable isotopes of helium, He-3, and He-4, and their mixtures, are the only macroscopic condensed matter systems that do not solidify at normal pressure even upon cooling to the absolute zero temperature. The cause for this is the large zero point energy compared to the interatomic bonds of the light noble gas. At extremely low temperatures the properties of the chemically identical isotopes differ considerably due to differences in quantum statistics. An especially interesting system is the dilute phase of the mixture of the isotopes, in which He-3 atoms form a rarefied fermi gas, whose properties can be continuously adjusted by varying the pressure and concentration, while the bosonic He-4 component remains in the background in the superfluid state. Also the He-3 component of the dilute mixture has been theoretically predicted to undergo a superfluid transition at very low temperature.

This thesis presents new methods for the experimental study of helium mixtures at very low temperatures, as well as results on measurements on the properties of helium fluids at previously unstudied temperature and pressure range. Adiabatic melting is a cooling method in which the cooling, based on the mixing of helium isotopes, is utilized in conditions where the heat capacity of the refrigerated system is falling fast, permitting a very low final temperature. In the first millikelvin-range trial of the new method, the mixture was cooled to 300 microkelvin temperature. This is not a particularly outstanding result compared to the traditional cooling methods, but the experiment was still encouraging as the limitations were found to be technical and no fundamental obstacles for improvements were discovered. The properties of the helium sample were studied by a sensitive pressure gauge, and by small immersed mechanical oscillators. Using these, the saturation solubility of the mixture was determined over the widest possible pressure range from zero to the melting pressure of the mixture. In addition the osmotic pressure of the mixture for several concentrations at the melting pressure was measured at millikelvin-range temperatures. Traditional vibrating wires and quartz tuning forks were used as the oscillators. Quartz tuning forks were found to be feasible sensors, though acoustic phenomena related to the high resonance frequency complicated the response.

Keywords helium-3, helium-4, helium mixtures, superfluid, melting pressure, solubility, osmotic pressure, dilution refrigeration

ISBN (printed) 978-952-60-4582-5

ISBN (pdf) 978-952-60-4583-2

ISSN-L 1799-4934

ISSN (printed) 1799-4934

ISSN (pdf) 1799-4942

Location of publisher Espoo

Location of printing Helsinki

Year 2012

Pages 174

The dissertation can be read at <http://lib.tkk.fi/Diss/>

Tekijä

Anssi Salmela

Väitöskirjan nimi

Kokeellisia tutkimuksia laimeiden heliumseosten ominaisuuksista matalissa lämpötiloissa

Julkaisija Aalto-yliopiston perustieteiden korkeakoulu**Yksikkö** O.V. Lounasmaa -laboratorio**Sarja** Aalto University publication series DOCTORAL DISSERTATIONS 43/2012**Tutkimusala** Kokeellinen materiaalfysiikka**Käsikirjoituksen pvm** 24.01.2012**Korjatun käsikirjoituksen pvm** 16.03.2012**Väitöspäivä** 27.04.2012**Kieli** Englanti **Monografia** **Yhdistelmäväitöskirja (yhteenveto-osa + erillisartikkelit)****Tiivistelmä**

Lähes absoluuttiseen nollapisteeseen jäähdetty helium on erittäin monipuolinen kohde kvanttiaineen kokeelliselle tutkimukselle. Heliumin kaksi pysyvää isotooppia, He-3 ja He-4, sekä näiden seokset, ovat ainoat makroskooppiset tiiviin aineen järjestelmät, jotka eivät kiinteydy normaalipaineessa edes nollalämpötilaan jäähdettäessä. Syy tähän on kevyen jalokaasun suuri nollapiste-energia verrattuna atomien välisiin heikkoihin vuorovaikutuksiin. Erittäin matalissa lämpötiloissa kemiallisesti samanlaisten isotooppien ominaisuudet poikkeavat hyvin paljon toisistaan, kvanttistatistiikan johdosta. Erityisen mielenkiintoinen järjestelmä on isotooppien laimea seos, jossa He-3 atomit muodostavat harvan fermikaasun, jonka ominaisuuksia on mahdollista muuttaa jatkuvasti painetta ja pitoisuutta säätämällä, bosonisen He-4:n ollessa taustalla perustilassaan. Teoreettisesti myös laimean seoksen He-3-osan on ennustettu muuttuvan supranesteeksi hyvin matalassa lämpötilassa.

Väitöskirjassa esitellään uusia menetelmiä heliumseosten kokeelliseen tutkimukseen matalissa ja erittäin matalissa lämpötiloissa, sekä mittaustuloksia seosten ominaisuuksista aiemmin tutkimmattomalla lämpötila- ja painealueella. Adiabaattinen sulatus on jäähdytysmenetelmä, jossa heliumisotooppien sekoittumisesta aiheutuvaa jäähtymistä pyritään hyödyntämään olosuhteissa, joissa jäähdytettävän systeemin ominaislämpökapasiteetin nopeasta laskusta johtuen hyvin matalan loppulämpötilan saavuttaminen on mahdollista. Uuden jäähdytysmenetelmän ensimmäisessä millikelvinalueella tehdyssä kokeessa seos onnistuttiin jäädyttämään noin 300 mikrokelviniin lämpötilaan. Saavutettu lämpötila ei ole erityisen hyvä verrattuna perinteisemmällä menetelmällä tehtyihin kokeisiin, mutta koe oli silti rohkaiseva, koska menetelmän rajoitukset osoittautuivat luonteeltaan teknisiksi eikä periaatteellisia esteitä tuloksen parantamiselle ole. Heliumnäytettä tutkittiin erittäin tarkkan painemittarin sekä pienten, nesteeseen upotettujen mekaanisten värähtelijöiden avulla. Näitä käyttäen kylläisen heliumseoksen pitoisuus mitattiin laajalla painealueella nollapaineesta seoksen sulamispaineeseen asti. Lisäksi osmoottinen paine sulamispaineessa mitattiin useille eri pitoisuuksille millikelvinalueella. Värähtelijöinä käytettiin sekä perinteisempiä värähteleviä lankoja että kvartsihaarukoita. Kvartsihaarukat osoittautuivat käyttökelpoisiksi antureiksi, joskin korkeaan resonanssitaajuuteen liittyvät akustiset ilmiöt monimutkaistavat vastetta.

Avainsanat helium-3, helium-4, heliumseos, supraneste, sulamispaine, liukoisuus, osmoottinen paine, laimennusjäähdytys**ISBN (painettu)** 978-952-60-4582-5**ISBN (pdf)** 978-952-60-4583-2**ISSN-L** 1799-4934**ISSN (painettu)** 1799-4934**ISSN (pdf)** 1799-4942**Julkaisupaikka** Espoo**Painopaikka** Helsinki**Vuosi** 2012**Sivumäärä** 174**Luettavissa verkossa osoitteessa** <http://lib.tkk.fi/Diss/>

Contents

Contents	i
Acknowledgments	iii
List of publications	v
Author's contribution	vii
1 Introduction	1
2 Refrigeration and thermometric methods	5
2.1 Motivation and short outline of established techniques	5
2.2 Adiabatic melting of ^4He crystal in superfluid ^3He at sub-millikelvin temperatures	6
2.2.1 Experimental setup	6
2.2.2 Results	9
2.2.3 Planned and implemented technical improvements	11
2.3 Vibrating wires and quartz tuning forks as sensors for helium liquids	14
2.3.1 Basis of the method	14
2.3.2 Practical implementation and results	16
2.3.3 Acoustic resonances in helium fluids excited by quartz tuning forks	18
2.4 Capacitive pressure gauge for melting pressure thermometry	22
2.4.1 Thermodynamical basis and technical realization	22
2.4.2 Results	23
3 Studies on properties of helium mixtures	25
3.1 Solubility of ^3He in ^4He at millikelvin temperatures	26
3.2 Osmotic pressure of $^3\text{He}/^4\text{He}$ mixtures	28

4 Conclusions	31
References	35

Acknowledgments

The experimental work was done in the YKI group at O.V. Lounasmaa Laboratory of Aalto University School of Science (formerly Low Temperature Laboratory of Helsinki University of Technology).

Guidance/collaboration by/with the following people is appreciated: Docent Juha Tuoriniemi, Dr. Alexander Sebedash, Professor Mikko Paalanen, Professor Pertti Hakonen, Professor Matti Kaivola, Dr. Elias Pentti, Juha Martikainen, Juho Rysti, and Matti Manninen. The care by the administrative personnel and the professionalism, expertise, and fine craftsmanship of the workshop and liquefier personnel is highly valued.

Funding by the Finnish Academy of Science and Letters: Vilho, Yrjö and Kalle Väisälä Foundation, and the National Graduate School in Materials Physics is acknowledged.

List of publications

This Thesis is based on the following original publications, which will be referred to by the respective Roman numeral.

- I** Anssi Salmela, Alexander Sebedash, Juho Rysti, Elias Pentti, and Juha Tuoriniemi, *Osmotic pressure of ^3He / ^4He mixtures at the crystallization pressure and at millikelvin temperatures*, Physical Review B **83**, 134510-1–8 (2011).
- II** A. P. Sebedash, J. T. Tuoriniemi, E. M. M. Pentti, and A. J. Salmela, *Osmotic Pressure of ^3He - ^4He Solutions at 25.3 Bar and Low Temperatures*, Journal of Low Temperature Physics **150**, 181–186 (2008).
- III** Elias M. Pentti, Juha T. Tuoriniemi, Anssi J. Salmela, and Alexander P. Sebedash, *Solubility of ^3He in ^4He at millikelvin temperatures up to the melting pressure measured by a quartz tuning fork*, Physical Review B **78**, 064509-1–13 (2008).
- IV** A. P. Sebedash, J. T. Tuoriniemi, S. T. Boldarev, E. M. M. Pentti, and A. J. Salmela, *Adiabatic Melting of ^4He Crystal in Superfluid ^3He at Submillikelvin Temperatures*, Journal of Low Temperature Physics **148**, 725–729 (2007).
- V** A. Salmela, J. Tuoriniemi, and J. Rysti, *Acoustic Resonances in Helium Fluids Excited by Quartz Tuning Forks*, Journal of Low Temperature Physics **162**, 678–685 (2011).
- VI** Anssi Salmela, Juha Tuoriniemi, Elias Pentti, Alexander Sebedash, and Juho Rysti, *Acoustic resonator providing fixed points of temperature between 0.1 and 2 K*, Journal of physics: Conference series **150**, 012040-1–4 (2009).
- VII** E. M. Pentti, J. T. Tuoriniemi, A. J. Salmela, and A. P. Sebedash, *Quartz Tuning Fork in Helium*, Journal of Low Temperature Physics **150**, 555–560 (2008).

-
- VIII** Elias Pentti, Juho Rysti, Anssi Salmela, Alexander Sebedash, and Juha Tuoriniemi, *Studies on Helium Liquids by Vibrating Wires and Quartz Tuning Forks*, Journal of Low Temperature Physics **165**, 132–165 (2011).
- IX** Alexander Sebedash, Juha Tuoriniemi, Elias Pentti, and Anssi Salmela, *Improved Capacitive Melting Curve Measurements*, Journal of physics: Conference series **150**, 012043-1–4 (2009).
- X** E. Pentti, J. Tuoriniemi, A. Salmela, and A. Sebedash, *Melting Pressure Thermometry of the Saturated Helium Mixture at Millikelvin Temperatures*, Journal of Low Temperature Physics **146**, 71–83 (2007).
- XI** A. Sebedash, J.T. Tuoriniemi, S. Boldarev, E.M. Pentti, and A.J. Salmela, *Melting Pressure Thermometry for Dilute ^3He - ^4He Mixtures*, AIP conference proceedings, **850**, 1591–1592 (2006).

Author's contribution

The publications this thesis is based on are results of predominantly experimental work carried out by the YKI group of the Low Temperature Laboratory. As part of the group, the author has had a varying contribution on the publications, depending on the division of tasks amongst the group members.

The measurements of publications **IV**, **X**, and **XI** and part of the measurements of publication **VIII** were done in one extended cooldown during which the author had an active role in the day-to-day maintenance of the experimental setup. The vibrating wire ensemble used for thermometry in these measurements was constructed by the author. Also, most of the data produced by the wires was initially analyzed by him.

Also the experiments treated in publications **I – III**, **VII**, and **IX** as well as part of the experiments displayed in publications **V**, **VI**, and **VIII** were conducted in one cooldown during which the author had a considerable contribution in running the experimental setup and to a smaller extent in performing the measurements. During the preparations of these experiments the author was actively involved in testing and building the components used in the setup, and had a considerable role in the final assembly of the setup as well.

Part of the experimental results of publications **V** and **VI** were collected among a wide range of minor experiments for which the author was responsible for constructing the experimental cell as well as planning and conducting the measurements.

The author was responsible for analyzing the experimental data for publication **I**, the draft of which was also written by him. Publications **V** and **VI** were written by the author.

During the span of this work our laboratory was also relocated, and the author had a major role in the disassembly, modification, transportation, reassembly, and testing of the advanced nuclear demagnetization cryostat the group is using.

Chapter 1

Introduction

Helium is the second lightest element and it has two stable isotopes, ^4He and ^3He , of which ^4He is the more abundant on earth. Because of the small mass and the complete electron shell structure of the atom, the interatomic bonds are weak compared to the zero point energy, which makes helium a unique system in several ways. At low temperatures, quantum mechanical effects are strong and govern the helium physics.

The stable helium isotopes, ^4He and ^3He , are the only condensed matter systems that stay liquid at absolute zero temperature, although solids too can be achieved but at considerably elevated pressures (2.536 MPa for ^4He and 3.439 MPa for ^3He). Also the boiling points are the lowest known (4.21 K for ^4He and 3.19 K for ^3He at saturated vapor pressure). Maybe the most thrilling property of helium liquids is superfluidity. For isotopically pure liquids the superfluid transitions at saturated vapor pressure occur at 2.177 K for ^4He and 0.93 mK for ^3He [1]. The great difference in the transition temperatures arises from quantum statistics. ^4He is a boson while ^3He is a fermion. Thus, pairing of ^3He atoms is required before a Bose-condensate like superfluid state can emerge, while ^4He atoms can form the condensate as such. The superfluid phases of pure isotopes have been studied intensively since their discoveries, reported in 1938 for ^4He [2] and 1972 for ^3He [3].

Helium mixtures are even more diverse systems than the pure isotopes. Below 0.87 K temperature (at saturated vapor pressure) the isotopes are miscible for only below and beyond certain temperature and pressure dependent proportions [1]. Even though the isotopes are chemically identical, the lighter ^3He occupies larger volume due to larger zero point motion, and thus the binding energy for any He atom is stronger in surroundings of ^4He atoms. Because of Fermi statistics and Pauli exclusion principle the effective binding energy of a ^3He atom

amongst the ^4He atoms decreases with concentration, until a value close to that of a pure ^3He system is reached, and a ^3He -rich phase will be formed. The available states for bosonic ^4He atoms are not limited by quantum statistics. So, the separated mixture has two phases: one rich with ^3He and the other rich with ^4He . The ^3He -rich phase is called simply the rich phase, and it becomes pure ^3He as temperature approaches zero. The phase with more ^4He in it is called the dilute phase and its ^3He concentration remains finite to absolute zero temperature.

The finite zero-temperature solubility makes the dilute phase a very special system. At millikelvin temperatures the ^4He component is in its ground state, and acts only as an inert environment for the fermi gas of ^3He quasiparticles. The effective mass as well as the interactions between the ^3He quasiparticles can be continuously adjusted by changing concentration and pressure. This tunable Fermi system is interesting already in itself, but the real bonus would be the theoretically predicted superfluid transition of ^3He in the dilute phase, resulting in a system of two intermixed superfluids. The non-zero concentration of the dilute phase is also vital for the operation of the widely used millikelvin cooling method, dilution refrigeration.

The search for experimental verification of superfluidity of the dilute phase has been going on, with varying activity, since it was first theoretically predicted in 1967 [4]. The theoretical estimate for the critical temperature T_c depends strongly on the mutual interactions of the quasiparticles, which are not precisely known and thus the predicted values for T_c vary a lot. The lower end of the estimates are clearly unattainable by any established cooling methods. Our measurements on the saturation concentration over a wide pressure range as well as measurements on the osmotic pressure of the dilute mixture at the melting curve can be used to estimate the interactions and to refine the T_c prediction. Our new estimate for the transition temperature of saturated mixture at the melting pressure is 40 μK [5].

In the past, dilute mixtures have been cooled to a temperature somewhat below 100 μK indirectly in a small sample volume connected thermally by a vast amount of sintered silver or platinum powder to a large copper nuclear stage combined with a powerful dilution refrigerator [6, 7, 8, 9]. Thermal Kapitza resistance, which increases drastically with lower temperatures, sets a practical limit for cooling helium by external means. Evidently, this limit has been reached in the experiments. A method acting directly on the helium mixture, such as adiabatic melting of ^4He solid in superfluid ^3He , is needed for further cooling. The method is basically a single-shot version of the dilution refrigerator that works below the superfluid transition temperature of ^3He . The isotopes are kept separated during pre-cooling by solidifying ^4He . After pre-cooling, the

isotopes are allowed to mix by melting the solid [10, 6, 11]. We have verified that the concept works at sub-millikelvin temperatures, but the full power of the process was not demonstrated due to technical restrictions **IV**.

Attaining extremely low mixture temperatures is challenging, but thermometry at this range is not trivial either. The high Kapitza resistance impedes thermalizing any separate thermometer with the fluid, and so the temperature must be determined by measuring some property of the fluid itself. The melting pressure of a helium crystal at certain concentration is related to temperature in a unique way. The melting pressure of ^3He at millikelvin temperatures is even used to define the lowest temperatures of the scale reaching the lowest temperatures agreed upon, albeit provisionally [12]. Also the melting pressure of ^4He solid in a mixture can be used as the basis for thermometry, especially in the case of univariant three phase state, where pressure depends uniquely on temperature **IX**, **X**, **XI**. Another widely used method for thermometry in this regime is to measure the dissipation caused by the excitations in superfluid ^3He by measuring the mechanical resonance characteristics of an immersed resonator. Traditionally small vibrating wires have been used as probes [13, 7], **VIII**, but lately also quartz tuning forks of different sizes have become common [14, 15], **VII**, **VIII**.

We observed strong unexpected anomalies in the tuning fork response, first in helium mixtures over a rather wide temperature range. Upon closer examination, we determined these features to be acoustic resonances that couple to the mechanical oscillator at certain conditions. We have observed first-sound resonances in pure ^4He and in helium mixtures at kelvin range, second-sound resonances of pure ^4He close to the superfluid transition and second-sound resonances of helium mixtures between 2 K and 30 mK **IV**, **V**. Even though the complicated geometry of the tuning fork resonator impedes real quantitative analysis of the situation, the resonance pattern can still yield some information on the properties of the medium. Also, it seems plausible that acoustic resonators could be utilized in some sort of a thermometric fixed-point device.

This thesis is based on several experimental studies on the properties of helium mixtures at low and ultralow temperatures. For the sake of composition, the experiments are divided in two groups. Articles **IV-XI** treat the problem from a more technical perspective, concentrating on the challenges of cooling the fluid and its thermometry, while on articles **I-III** the emphasis is more on the basic research on helium. The division is not strict, the more technical publications still involve helium physics and vice versa.

Chapter 2

Refrigeration and thermometric methods

2.1 Motivation and short outline of established techniques

Experimental techniques used in low temperature research have advanced significantly since Heike Kamerlingh Onnes first liquefied helium in 1908. Now liquid helium can be manufactured on industrial scale. The commercially available helium liquid (4 K) can be used as a starting point for reaching lower temperatures in steps relying on widely used and well-polished methods of helium evaporation refrigeration (down to 1.2 K), dilution refrigeration (reaching relatively easily 20 mK, with a record at below 2 mK), and adiabatic nuclear demagnetization cooling (below 100 μ K). In the past ten years, pulse tube cryocoolers have been combined with dilution units to make dry cryostats that can be operated without notable expertise in low temperature techniques, to reach temperatures below 20 mK.

In spite of all the technological progress in cooling techniques, for research efforts where certain substances are desired to be cooled to extremely low temperatures, the existing cooling methods are not sufficient. One such system is liquid helium. Pure ^3He and the mixture of helium isotopes offer interesting physics to be discovered at temperatures far below 1 mK. We have experimented with a method, adiabatic melting, in which cooling by dilution is started at very specific starting conditions. The method is described in section 2.2, together with the obtained results.

The latest official temperature scale, ITS-90, defines temperatures from the highest values practically measurable by Planck radiation law down to 0.65 K. For the low end of the scale (3 K - 0.65 K), helium vapor pressure-temperature relations are used to define the temperatures [16]. The extent of the ITS-90 scale is clearly too narrow for most low-temperature research. Thus, a provisional temperature scale PLTS-2000 has been agreed upon. PLTS-2000 uses the melting curve of ^3He , with fixed points at superfluid A and A-B transitions as well as the Néel point of the solid, to define temperatures from 1 K down to 0.9 mK [12]. This range is already adequate for most low temperature investigations, but the practical realization of the melting curve measurements is experimentally demanding.

This thesis describes melting curve measurements for pure ^4He solid in saturated helium mixture using an extremely sensitive capacitive differential pressure gauge. Results from these measurements are reported in section 2.4. We have also used small mechanical oscillators to investigate the properties of helium fluids. The use of small resonators for thermometry at millikelvin range is discussed in section 2.3.

2.2 Adiabatic melting of ^4He crystal in superfluid ^3He at sub-millikelvin temperatures

2.2.1 Experimental setup

Adiabatic melting of ^4He crystal in superfluid ^3He is a way to cool helium mixtures by using the entropy difference of ^3He atoms in the pure and dilute phases [10, 11], **IV**. As the cooling takes place directly in the liquid, the method is especially suitable in experiments where helium itself is the subject of the studies.

The entropy diagram of ^3He in pure and dilute phases is shown in figure 2.1 [6]. For each ^3He atom the molar entropy is smaller in the pure phase and so mixing the isotopes causes cooling if the process is adiabatic. The entropy of the pure phase rapidly decreases as ^3He turns superfluid, which increases the entropy difference and also the cooling factor $x = T_{\text{initial}}/T_{\text{final}}$. For a regular dilution refrigerator, which operates above T_c , the cooling factor is about three, but if the temperature where the mixing is started can be reduced to below T_c , the cooling factor can reach orders of magnitude larger values.

The cooling power of the method is determined by the heat of mixing the isotopes which is proportional to the temperature and the entropy difference of

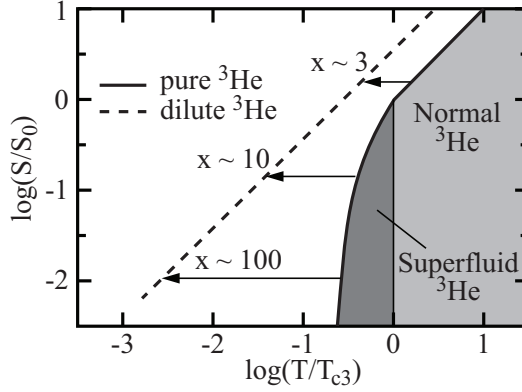


Fig. 2.1 Molar entropy of ^3He in pure and dilute phases. The arrows indicate perfectly adiabatic transitions from different starting temperatures, resulting in cooling factors $x = T_{\text{initial}}/T_{\text{final}}$.

the pure and dilute phases. As both phases are degenerate Fermi systems with entropy depending linearly on temperature, the temperature dependence of the cooling power will be quadratic.

$$\dot{Q} = T\dot{S} \approx 100\dot{n}T^2, \quad (2.1)$$

where \dot{n} is the molar rate of transferring ^3He from the pure to the dilute phase. The numerical factor 100 is not exact and originates from the difference of enthalpies (specific heats) of the pure and the dilute phases [1]. For a rate of $100 \mu\text{mol/s}$ at $100 \mu\text{K}$ temperature, the cooling power is 100 pW . The small and rather swiftly decreasing cooling power sets strict limitations for the technical implementation of the experiment: All sources of heatleaks must be eliminated so that the dilution process stays as adiabatic and reversible as possible.

The adiabatic melting experiment was performed in the cell illustrated in figure 2.2 IV. The cell was installed in a powerful nuclear demagnetization refrigerator with a base temperature of less than 0.1 mK [17]. The inner structure of the cell is made of annealed high purity copper with sintered silver powder covering the upper half of the inner surface to increase the thermal contact to helium. The softer inner cell is supported by a bulky bronze encasing to make the cell very rigid so that changes of pressure do not cause deformations and dissipation.

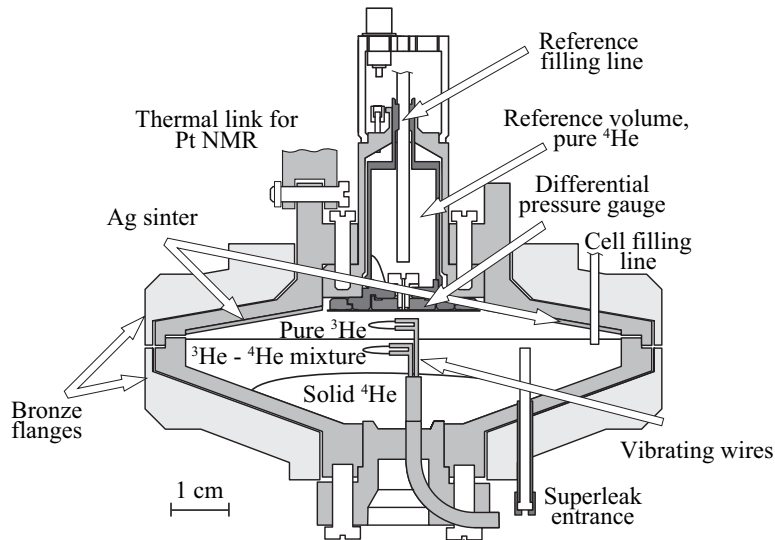


Fig. 2.2 High pressure cell used in the adiabatic melting experiment.

Also the general saucer-like shape is selected to avoid viscous heating as fluids relocate during melting. The total volume of the cell is 78 cm^3 .

The main volume of the cell is equipped with two inlets, one normal and one a so-called superleak, which is vital for the execution of the experiment. The superleak is a Cu-Ni capillary tightly packed with powder so that there is no free volume inside the capillary, just a very constrained porous medium. The superleak has two important properties: it allows only superfluid to permeate, and the melting pressure of ^4He in the constrained geometry of the superleak is higher than in free volume [18].

The temperature of the cell wall was measured by a platinum NMR thermometer, while the state of the helium phases was monitored by two vibrating wire resonators. The pressure of the cell was measured by a differential capacitive pressure gauge installed directly on top of the cell. A partially solid pure ^4He sample was used to provide the reference pressure. The resolution of the gauge at the melting pressure of ^4He in the mixture was 0.01 Pa **XI**.

The experiment progressed so that the cell was filled with mixture using the normal capillary. Optimally, the proportions of the isotopes are selected so that

upon pressurizing and the consequent solidification of ^4He , all ^4He in the cell would be in the solid, resulting in perfectly separated pure ^3He and ^4He phases. When the ^4He solid is grown in the mixture at a temperature below 50 mK, it will be practically isotopically pure [19]. The pressure was controlled by the superleak, while the normal capillary was blocked by solid. After the isotopes were separated by solidifying the ^4He , the cell was precooled by the nuclear demagnetization stage. When the fluid temperature had reached 500 μK , melting of the solid was initiated. Solid was melted by extracting ^4He through the superleak. During melting, as long as solid ^4He was present, the pressure of the cell remained nearly constant. As the molar volume of the liquid phase is roughly 10% higher than that of the solid phase extracting an amount of ^4He out of the cell released about tenfold amount of liquid ^4He in to the cell that mixed with ^3He resulting cooling.

2.2.2 Results

We made one cooldown with the complete adiabatic melting setup, during which cooling by melting was tried several times. Up to date, these tests are the only instances when an adiabatic melting experiment has been attempted at millikelvin range temperatures. In the attempts, the method was proven to be viable, but technical complications prohibited the demonstration of its full potential. Four instances of the melting process are illustrated in figure 2.3. The technical limitations and the planned improvements are discussed in section 2.2.3

The first example is labeled with 'a' in figure 2.3 **VIII**. The melting was initiated at about the three-hour mark, but soon this had to be suspended since the cell wall, as well as the liquid, started to rapidly warm up. After few hours of settling, melting was tried again (twice), with a lower extraction rate. Now a clear decrease in the liquid temperature was seen at first, but then the cell wall and eventually also the liquid started to heat up. At about 8 hours, the melting was started again, and now extraction of ^4He could be continued without heating effects and the extraction rate was increased in steps resulting in corresponding decreases in the liquid temperature, until the cell wall heating again ruined the run when the rate was raised to 40 $\mu\text{mol/s}$. It was evident, from the order the thermometers in different places in the cryostat reacted to the temperature rise, that the heating started in the superleak and far away from the cell.

In case 'b', the melting is continued for a long time with a low extraction rate. The small rate was sufficient to bring the liquid temperature to that of the cell wall. The temperature difference was restored when the melting was stopped after 20 hours.

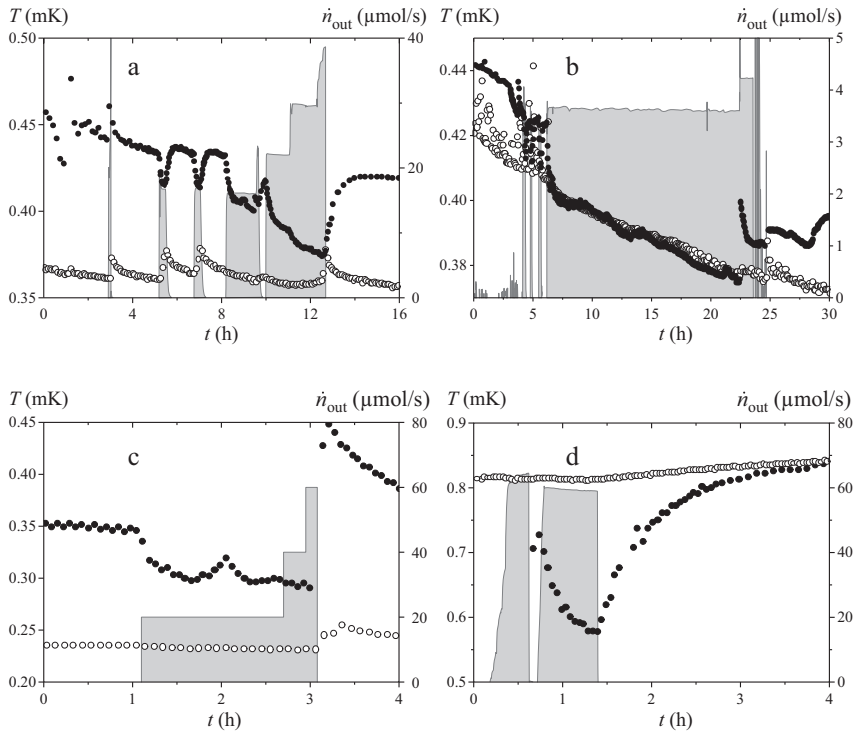


Fig. 2.3 Four examples of the adiabatic melting cooling, see text for details. The temperature scale is shown on the left. The sample temperature, measured by a vibrating wire in pure ^3He phase is shown by the filled symbols and the temperature of the cell wall by the open ones. The filled gray area shows the flow through the superleak, the scale being given on the right. The time axis shows the time in hours from an arbitrary point close to the start of melting attempt.

In case 'c', the initial temperature was the lowest. At this temperature range, the resonance width of the vibrating wire is already close to being saturated to the vacuum value and is not reliable as an absolute thermometer, but still can be used as an indicator for temperature changes. Also in this case, the temperature of the liquid can be reduced by melting the solid until the point when the extraction rate became too high and heating resulted. The lowest temperature of the liquid was roughly 300 μK , which is not a particularly outstanding result. With the more traditional way of cooling the liquid through a large amount of sinter refrigerated by a nuclear demagnetization refrigerator, temperatures below 100 μK have been reached [9, 6]. The difference is that we believe that the about 100 μK temperature is the limit for the traditional method, whereas the performance of the adiabatic melting has significant potential for improvements by technical means.

The last case 'd' shows an occasion when we managed to cool the liquid below the cell wall temperature. This attempt was done at a higher temperature, which enhanced the cooling power compared to cases 'a' to 'c'. The first melting slightly exceeded the critical ^4He extraction rate which caused liquid to warm up. At this high temperature only a few minutes' wait was needed before the second attempt was started and the liquid cooled below the temperature of the cell wall.

The melting of case 'd' also resulted in the highest cooling factor of 1.4. This is orders of magnitude less than the theoretically anticipated values. The large deficiency can be explained by a simple thermal model taking into account the nonidealities of the starting condition and the technical restrictions of the experimental setup, see publication **IV** for details.

2.2.3 Planned and implemented technical improvements

We learned about several technical hindrances during the first cooldown with the complete adiabatic melting setup. Heating from operating the superleak, and measuring the state of the helium sample, as well as heatleaks from the structures of the cell made the process of mixing the isotopes nonadiabatic. In addition, the smaller than expected throughput of the superleak limited the cooling power.

The old superleak line has since been rejected and several new ones manufactured and tested. The old line was constructed of three separate sections with small thermally anchored joints in between, whereas the new lines are continuous. In the tests, the new lines were found to allow the planned 100 $\mu\text{mol/s}$ flow through without observed heating effects anywhere in the line, but new problems were discovered. There was an occasional effect which caused rapid

pressure fluctuations and a strong oscillating flow in the lines. We believe that this was related to a normal fluid superfluid interface at about 2 K location of the line. To avert this, the most vital superleak line was be disconnected altogether from high temperature parts of the system by a specially made bellow system.

The bellow system consists of two adjustable volume chambers, mechanically connected in a way, which allows one chamber to be used to vary the volume and pressure of the other one. The upper bellow is planned to be at above 2 K temperature, and its volume will be controlled by pressure from a room-temperature gas handling system. The lower bellow is meant to be at below 10 mK temperature, filled by helium mixture and connected to the adiabatic melting cell by a superleak. The upper bellow can be used to manipulate the lower bellow to shift ^4He to and from the cell as the melting experiment is conducted. The bellow system has already been built and the mechanical operation tested.

Another problem, and a somewhat surprising finding, was that the thermal contact between the inner cell wall and the liquid inside is actually too good. This limited the performance since part of the cooling power from the mixing of the isotopes was wasted on the cell structures (in the rare occasions when the liquid was actually colder than the walls). To fix this, the cell has been divided in to two parts, one being a smaller volume with the sinter and second containing the main bulk of the helium sample. The two parts will be connected by a capillary equipped with a cold valve. During precooling the valve is open to let the main volume thermalize to the wall temperature, while as melting is started the valve will be closed to isolate the helium sample from the cell structures. To reduce the thermal load to the cell, the outer reinforcement structure material is changed from bronze to copper.

Thermometry at these temperatures is always a considerable problem. We had difficulties with diminishing sensitivity as well as with the heating generated by the measurements. The issues regarding the tested thermometers are discussed in the next two chapters. We have also a plan to include two new means to measure the liquid temperature: Pt-NMR and noise thermometers. These devices do not measure the liquid temperature directly, but have sensing elements that must be thermalized with the liquid and thus may have a long response time and limited usability at very low temperatures.

A schematic figure of the complete setup, with the proposed improvements, for the adiabatic melting experiment is shown in figure 2.4.

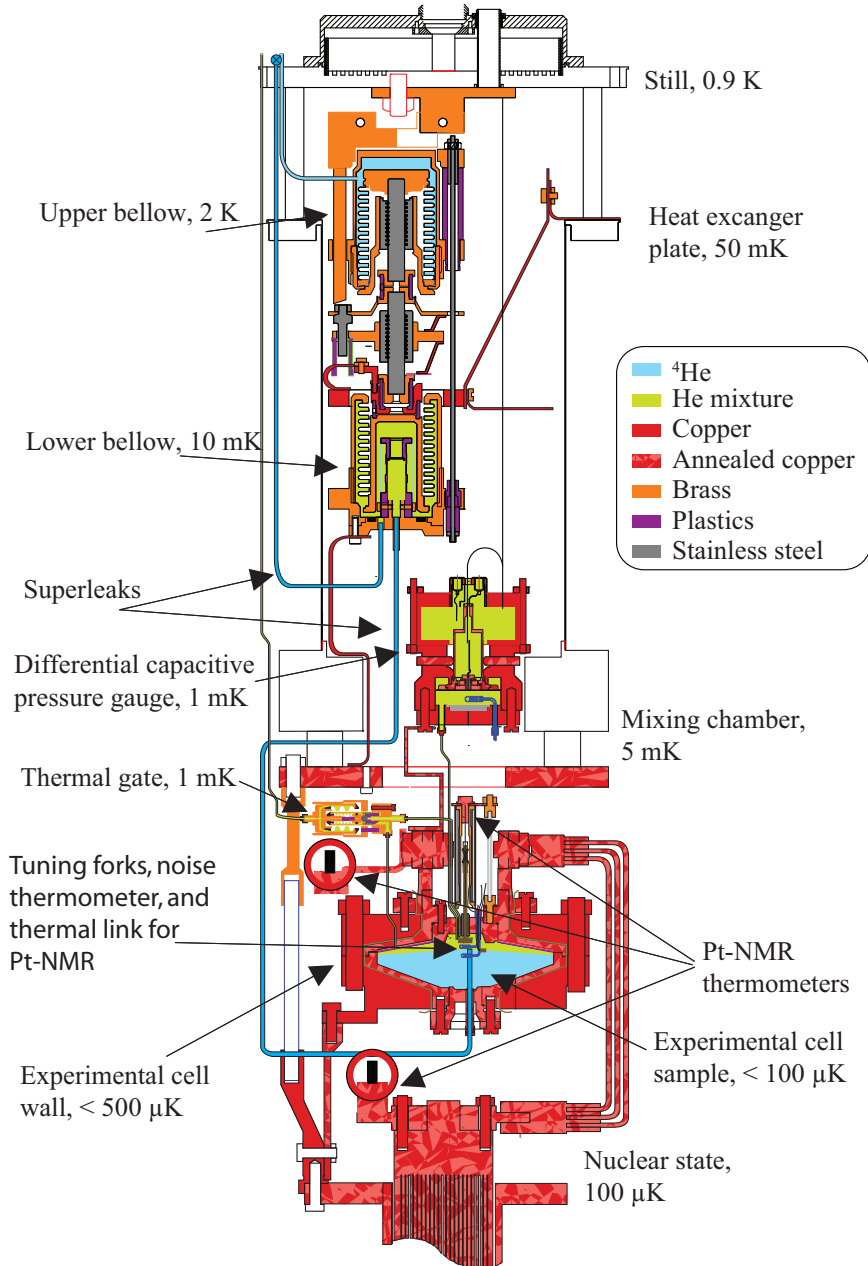


Fig. 2.4 Experimental setup for the adiabatic melting experiment.

2.3 Vibrating wires and quartz tuning forks as sensors for helium liquids

2.3.1 Basis of the method

Small vibrating objects, such as wires [13, 7], **VIII**, grids [20], levitating spheres [21], and lately also tuning forks [14, 15], **VII**, **VIII**, are a standard tool in the study of helium fluids at low temperatures. These sensors can be treated as harmonic oscillators, driven electrically near an eigenfrequency f_0 and damped by the medium. The damping force has dissipative and dispersive components that depend on the properties of the fluid. The force acts as effective inertia and loss that are seen as a shift in frequency and an increase in the half width of the measured resonance w . The effect of the damping force on the motion of the oscillator is inversely proportional to the inertia of the oscillator, and so the sensitivity can be tuned by varying the density and dimensions of the oscillator.

Different models can be used to describe the damping force depending on the mean free path ℓ of the excitations. For some regimes, analytical solutions can be calculated for simple geometries [22], but generally complicated numerics must be applied to solve the force [23, 24]. Most experiments were done in Fermi liquids (pure ^3He and helium mixtures at low temperatures) where ℓ for the quasiparticles ranges from almost zero to infinity as temperature decreases. The increase with decreasing temperature is due to the Pauli exclusion principle that strongly limits the allowed final states of quasiparticle-quasiparticle scattering.

At relatively high temperatures, when the mean free path is short compared to characteristic experimental dimension a , hydrodynamic model applies. The fluid can be considered as a continuum, described by density ρ and viscosity η , and also acoustic phenomena are possible. At the limit $\ell/a \rightarrow 0$ the fluid is ideal, and produces no resistance to the motion of the oscillator. In the hydrodynamic range, the damping force for an infinitely long cylinder was solved analytically by Stokes. The force depends on the viscous penetration depth $\delta = \sqrt{\eta/(\pi\rho f)}$ [25]. The viscosity η of a Fermi liquid is roughly proportional to T^{-2} which leads to a power-law behavior for the resonance width with an exponent between 1..2, depending on the frequency and geometry. The increase of viscosity causes the resonance frequency to decrease as more fluid is dragged along with the resonator.

A rising ℓ first begins to cause deviation from the purely hydrodynamic behavior, which can, to some extent, be taken into account by the so-called slip corrections [25, 26, 27, 28, 29]. When ℓ becomes large compared to a , the quasiparticle gas

needs to be described as a collection of ballistic particles and such concepts as viscosity or conductivity are not valid any more. As ℓ increases, the probability that a once-scattered quasiparticle will again transfer momentum with the oscillator will fall. The number of quasiparticles and the rate of scattering processes stay constant, but the phase correlation between the quasiparticle gas and the oscillator will weaken. This causes an increase in the resonance frequency since the mass of the quasiparticle gas decouples from the oscillator. On the other hand, the resonance width (dissipation) increases as the separation of momenta of the oscillator and the average incoming quasiparticle increases.

In the fully ballistic regime, as $\ell \rightarrow \infty$, the force acting on the resonator will saturate to a value proportional to the quasiparticle density, the Fermi momentum as well as to some geometrical factors [28]. The force is in phase with the velocity of the oscillator and is thus purely dissipative and only causes widening of the resonance but no shift in frequency, so the resonance frequency is expected to be determined by the density of the ^4He component. In experiments of Ref. [30], the resonance frequency is observed to rise even higher than the value corresponding to the density of the ^4He background. The result is reproduced in numerical calculations [24]. There are several contributions to this overshoot: part of the bosonic ^4He atoms are coupled to fermions and they also decouple from the oscillator. There is an elastic restoring force rising from the dynamics of the Fermi liquid that increases the resonance frequency, and the reflected quasiparticles cause an effect when the finite geometry of the experimental volume is taken into account [23].

For pure ^3He , the behavior changes drastically at T_c as the number of quasiparticles starts to decrease rapidly as they form Cooper pairs that condense to a superfluid state. Near T_c the damping force has a complicated temperature dependence [31], but at sufficiently low temperatures in superfluid $^3\text{He-B}$, the damping follows a rather simple exponential decay law $e^{-\Delta/k_B T}$, where Δ is the superfluid energy gap and k_B the Boltzmann constant [32].

We made some tests also in ^4He , which is not a Fermi liquid and so the above discussion does not apply. The situation is still quite similar. At high temperatures, that for the case of ^4He mean temperatures above 2.2 K, the mean free path is small and the fluid behavior is hydrodynamic. Below the superfluid transition temperature $T_\lambda = 2.17$ K, the number of excitations starts to decrease rapidly and damping drops. Below about 1 K the normal fluid fraction is negligible, and scattering, dominated by thermal phonons, decreases as T^4 [15].

2.3.2 Practical implementation and results

Vibrating wires are usually semicircular in shape, driven by Lorentz force of a small AC-current in magnetic field, and the motion is detected as the induced voltage. In the first try of adiabatic melting experiment, we used two vibrating wires to study the sample. The wires were located so that the upper one was in the pure ^3He phase and the lower one in the mixture. The insert to the bottom flange of the cell is shown in figure 2.5. The demands for a resonator differ depending on which regime and to what purpose it is intended to be used. Quite generally, maximizing the Q-value (f_0/w) in the extreme experimental conditions is preferable.

The upper resonator was used for thermometry in superfluid $^3\text{He-B}$ well below T_c . For this purpose the wire should be highly sensitive to the effect of the low damping medium. Sensitivity was increased by making the wire light, which can be achieved by using low density material and small dimensions. The wire was made of 50 μm diameter single filament superconducting NbTi wire (exact composition unknown, the approximated density of which was $\rho = 5.5 \text{ g/cm}^3$ VIII). The resonance frequency in vacuum depends on the material and geometry for the upper wire it was 1050 Hz. The factor that ultimately limits the low-temperature sensitivity is the intrinsic damping, which defines the resonator's vacuum resonance width. The intrinsic damping depends on the losses that take place within the resonator itself, and those can be minimized by material choices and careful construction. The low-temperature vacuum width was 160 mHz, quite a lot more than expected. Also the width had a clear temperature dependence extending down to low millikelvin temperatures. NbTi is not the optimal choice for the wire material regarding neither of the requirements. For instance, Al is lighter and as a pure metal also dissipates less internally. NbTi was chosen for practical reasons, as the higher superconducting transition temperature eased testing the wire construction prior to installation.

The lower wire was used to monitor the state of the mixture phase, the main function being to detect the possible superfluid transition of the dilute phase. For this intent, high sensitivity and narrow vacuum width are not that vital as the damping caused by the fully ballistic helium mixture is very large. The dimensions of the wire had to be selected so that the Q-value remained relatively high in all conditions to allow for resolving the resonance curve with reasonable excitation. Thus a thicker and more dense wire was used, to both slightly increase the vacuum resonance frequency and to decrease the impact of the highly dissipative fluid on the resonance width. The resonator was made of 125 μm diameter Ta wire ($\rho = 16.7 \text{ g/cm}^3$). The vacuum resonance frequency was ca.

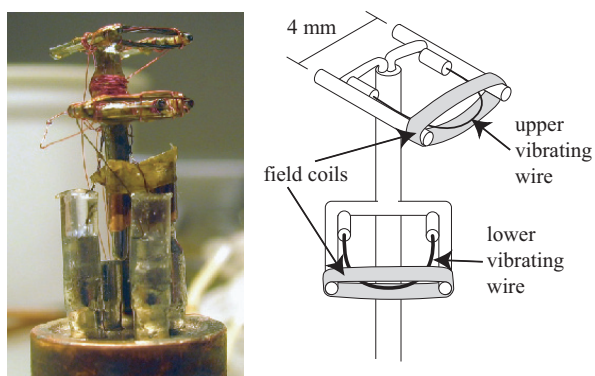


Fig. 2.5 A photograph and a schematic drawing of the vibrating wire resonator insert used in the adiabatic melting experiment. The upper wire is made of 50 μm diameter NbTi and the lower of 125 μm Ta filament.

2500 Hz, and the resonance width saturated to about 200 Hz in the mixture at the lowest temperatures ($Q\text{-value} \approx 10$).

One additional complication was that the obligatory magnetic field had to be generated locally, since the whole cell could not be in the static magnetic field for heat capacity reasons. For this purpose, small flat superconducting coils wound around the wires were used. The coils made the wire construction somewhat cumbersome, which may have had an effect on the intrinsic damping (vacuum width) by increased dissipation at the support points at the ends of the wire.

Quartz tuning forks are mass produced resonators used in consumer electronics as frequency references, and they usually operate at $2^{15} = 32768$ Hz frequency in vacuum at room temperature. Quartz is piezoelectric so that excitation and detection are done regardless of magnetic field. The piezoelectric voltage rising from the fork's motion is also larger than the induced voltage on vibrating wires obtained with feasible magnetic fields. The low density of quartz ($\rho = 2.65 \text{ g/cm}^3$) increases the sensitivity in all regimes in comparison with vibrating wires of similar dimensions. On the other hand, the higher resonance frequency decreases the viscous penetration depth and decreases sensitivity in the hydrodynamic range. This is actually an advantage since the $Q\text{-value}$ remains higher in the highly viscous media but the sensitivity is not influenced in the low damping conditions of ballistic superfluid. For some selected types of forks, the crystalline structure is also of very high quality, allowing very narrow vacuum resonances of only few mHz in width with no temperature dependence

at low temperatures. It seems plausible that forks can be used for thermometry to temperatures below 100 μK .

In the planned next adiabatic melting experiment, four tuning forks are going to be used. Two of them are in the actual experimental cell and two more are in the detached pressure gauge. To reduce the possible interference problems, all four forks will operate at different frequencies. The most critical fork is the one that is to be used for thermometry in the pure ^3He phase in the cell. For this we will use fork model ECS 1x5x, operating at 32768 Hz which has proven to be very good in terms of low internal damping in our experience. The fork in the mixture phase in the cell will be operating at 20.0000 kHz (Epson C-2 20.0000K-P). The two other forks will be in the pressure gauge, a 32.9190 kHz fork (Epson C-2 32.9190KC-P) in the reference volume and a 40.00 kHz fork (ECS-.400-12.5-13) in the primary volume. An image of a Fox Electronics model NC38 tuning fork is shown in figure 2.6 **VI**, **VIII**. Forks of different models and manufacturers have the same general geometry, but the sizes may differ.

Forks seem to ease all the problems discovered in vibrating wire measurements during the adiabatic melting experiment, but there are also some disadvantages. The more complicated geometry makes analytic calculation of the damping force impossible, and the numerical approach is also more cumbersome. For instance, in the hydrodynamic range the response of the resonance width in helium mixtures is not T^{-1} as for wires, but close to $T^{-3/4}$, which is not compatible with the Stokes solution for an infinitely long cylinder. The order of magnitude higher resonance frequency also introduces complications related to acoustic phenomena. These will be discussed in the next section. The smallest forks are also larger in size than the smallest vibrating wires, which can present a problem in some applications.

2.3.3 Acoustic resonances in helium fluids excited by quartz tuning forks

While conducting tests for the detached pressure transducer and the new superleaks, we also had a tuning fork (model NC38) installed in the pressure gauge volume. We measured the fork response using so called single point method, in which the a single measurement at a frequency near the resonance frequency is used to calculate the resonance characteristics assuming Lorentzian lineshape with known area and background **VIII**. As the experiments described in chapter 3 progressed and the first doses of ^3He were added among the ^4He already in the volume, strong anomalies in the fork response were observed. The apparent res-

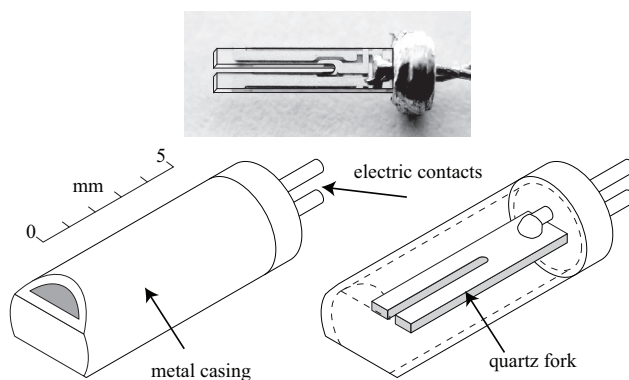


Fig. 2.6 A photograph and schematic drawing of a quartz tuning fork (Fox Electronics NC38). The outline of the fork in the photograph has been enhanced by drawn lines. The basic geometry is similar also for the smaller fork models used.

onance width was seen to widen considerably at certain temperatures. We have concluded that these features are a result of standing acoustic waves coupled to the tuning fork. Later, we have observed them in various helium fluids, namely: supercritical ^4He , normal fluid ^4He , superfluid ^4He , and helium mixtures.

Of the acoustic modes known in helium fluids (zeroth, first, second, third, and fourth sounds) the first- and second-sound can exist in bulk helium fluids at the conditions we have studied. The first-sound is the ordinary transverse pressure wave that exists in the hydrodynamic regime. For pure ^4He liquid at SVP, the first-sound velocity increases from about 170 m/s at the boiling point through a notable kink at T_λ and saturates to about 240 m/s below 1 K. For helium mixtures at the same temperature range, the velocities are slightly smaller. For supercritical helium fluids the sound velocity varies considerably, mostly depending on the pressure. The second-sound is an acoustic mode specific to superfluids. It can be described as an entropy wave, where the excitations and the superfluid component move in opposite phases, while the pressure of the whole fluid stays constant. The excitations can be either the normal component if superfluids are studied at finite temperatures, or ^3He quasiparticles in the case of helium mixtures. In helium mixtures the second-sound velocity varies from little below 10 m/s to about 40 m/s depending on pressure, concentration, and temperature. For pure ^4He the second-sound velocity increases from zero at T_λ to over 40 m/s before the whole acoustic mode ceases to exist below 0.7 K as the normal component vanishes. For an acoustic mode to couple to the resonator, a standing

wave must be excited in the cavity in the vicinity of the resonator. This means that the wavelength of the excited mode must match a dimension of the resonator or the experimental volume. For typical fork dimensions (millimeter scale) and resonance frequency (32 kHz), the required sound velocity should be of the order of 30 m/s, which agrees with the velocities for the second-sound. Forks can also be operated at a higher harmonic frequency (200 kHz), which matches resonant modes at the first-sound velocities.

We studied the acoustic resonances in various helium fluids by either recording rather wide frequency sweeps while the sound velocity was changing slowly or by making the measurement at a single frequency and determined the resonance characteristics from this as explained in publication **VIII**. A sample of results of the first method is shown in figure 2.7 **V**, where acoustic modes in supercritical ^4He are shown. The plot indicates the dynamics of a system of coupled resonators, with varying strength of coupling of the passing acoustic modes.

In the single point method, the area under the resonance curve is assumed to stay constant, which does not hold when the acoustic mode is coupled to the fork as the energy introduced to excite the fork is distributed over the distinct modes. Still, if the resonance pattern is not overly complicated, the single point method can give a reasonable account on the resonance frequency of the mechanical resonator, while it crudely exaggerates the width. In figure 2.8 **V** the apparent resonance frequency and width over a wide temperature range for about 8% mixture is shown. The very sharp distinguishable features, with high temperature resolution, in the apparent resonance width could possibly be used as fixed points, as proposed in publication **VI**.

Acoustic losses, related to the second-sound, can also be one reason for the peculiarly slow decrease of the damping in helium mixtures as function of temperature in the hydrodynamic regime. Especially since the deviation from the Stokes theory is observed solely in mixtures, and pure ^3He behaves as expected, so some connection to the existence of the second-sound seems probable.

In general, acoustic resonances are usually just a nuisance. They cause rather strong effects and are difficult to predict. To escape from them the resonance condition should be avoided. This can be done either by changing the measurement frequency or the experimental dimensions. For measurements in helium fluids at millikelvin temperatures smaller resonators with lower frequencies should be used.

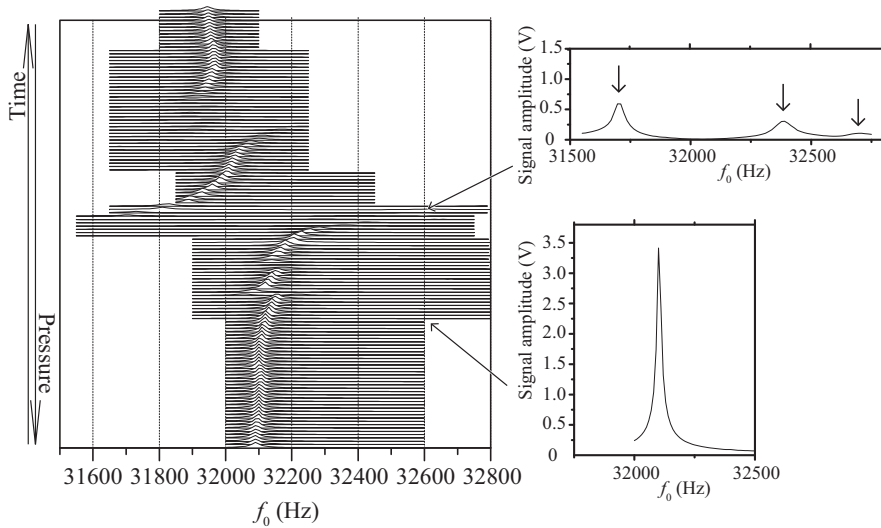


Fig. 2.7 Acoustic resonances in supercritical ^4He . The spectra were recorded at the constant temperature of 4.6 K while the pressure decreased from 0.26 to 0.21 MPa in 8 hours. The two inserts show example spectra in situations where no acoustic modes are present (lower frame) and where two acoustic modes are coupled to the mechanical oscillator (upper frame).

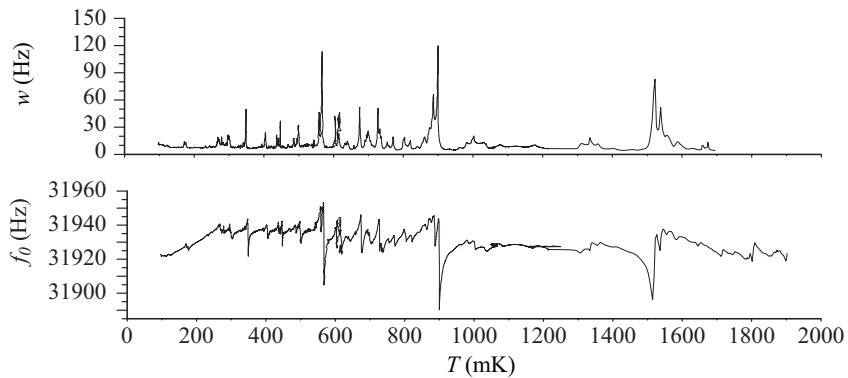


Fig. 2.8 Apparent resonance width and frequency, determined by the one point method (see publication **VIII**), in about 8% helium mixture as a function of temperature.

2.4 Capacitive pressure gauge for melting pressure thermometry

2.4.1 Thermodynamical basis and technical realization

We have used the temperature dependence of the melting pressure of ^4He crystal in saturated helium mixture for thermometry at millikelvin temperatures. When the phase separated mixture is pressurized, three phases will result, dilute liquid mixture, rich liquid mixture, and dilute solid. If pressurizing is done at a temperature below 50 mK, the three phases will be pure ^4He crystal, pure ^3He liquid, and liquid saturated mixture. These phases form a univariant state, in which the melting pressure is uniquely defined by temperature [19].

The slope of the melting curve is given by the Clausius-Clapeyron relation

$$\frac{dP}{dT} = \frac{\Delta s}{\Delta v}, \quad (2.2)$$

where Δs is the difference in entropy, and Δv the difference in the molar volume of the liquid and solid phases. At the low-temperature limit the temperature dependence of the melting pressure of a helium system is essentially defined by the entropies of the phases present, since the molar volumes have saturated to constant values. For the above described univariant state, entropy of the solid phase is negligible and thus a temperature-independent constant. The two liquid phases are Fermi systems with entropies directly proportional to T above superfluid transitions, so the melting pressure follows a simple quadratic temperature dependence. In comparison to the melting pressure of pure ^3He , the low-temperature limit of the slope of the melting pressure curve is the opposite, since in pure ^3He a larger part of the entropy is in the solid. The form of the temperature dependence for the system is also considerably simpler, especially above T_c , and the sensitivity at a very low temperature is higher than in pure ^3He .

At T_c of the pure phase, analysis becomes more complicated as the entropy of the pure phase starts to drop exponentially in T , which causes the melting curve to drop faster than T^2 in the temperature range where the superfluid has any significant contribution to the entropy of the system. At temperatures much lower than T_c , the melting pressure is again quadratic in T , until the superfluid transition of the dilute phase. A more complete theoretical analysis of the three phase system is presented in publication **X**.

The melting pressure was measured using a capacitive differential pressure transducer. The sensing element was made of 0.2 mm thick BeCu foil with 29 mm

diameter, which formed one electrode of the capacitor used to measure the deflection of the foil. The pressure was measured against a reference pressure of the same order, so that the membrane could be made thinner to increase sensitivity. The same sensor was used to measure the pressure difference of the experimental chamber and the reference volume in the adiabatic melting experiment as well as in the tests with the detached pressure gauge described in chapter 3. In both experiments, partially solid pure ^4He was used as the reference medium. An Andeen-Haegerling AH 2500A capacitance bridge was used for the capacitance measurement.

2.4.2 Results

The same differential capacitive pressure sensor was used in two setups, in the adiabatic melting cell, and in the detached pressure gauge. The mixture pressure was always measured against the melting pressure of pure ^4He (2.53 MPa) which defined the magnitude of the absolute pressures. In both cases the performance of the sensor was similar. During the melting curve measurements, capillaries to both volumes, main and reference, were blocked by solids at about 1 K temperature to disconnect them from higher temperature fluctuations.

The pressure gauge can be considered as a parallel-plate capacitor with the gap decreasing in proportion to the pressure increase. The relation of the capacitance and pressure is $C(p) = C_0(1 - p/p_s)^{-1}$, where C_0 is the capacitance at rest position and p_s the pressure when the capacitor plates will short. For the gauge, C_0 was about 8 pF and p_s about 41 kPa. The melting pressure of the saturated mixture is about 34 kPa above the reference of the melting pressure of pure ^4He . At this pressure difference the sensitivity of the gauge was about 3.4 fF/Pa. The measured peak-to-peak fluctuation of the capacitance measurement was about 20 aF, which results in a pressure resolution of about 6 mPa at the pressure range of interest. In publication **X** the slope of the melting curve for the univariant system below T_c is found to be 1.52 Pa/mK². This implies that the resolution of the pressure gauge should allow for thermometry at temperatures below 100 μK .

The resolution of the pressure transducer was so high that some not so obvious factors influencing the measured melting pressure had to be taken into account, when analyzing the results. The hydrostatic pressure of the liquid between the solid-liquid interface on the bottom of the cell and the pressure gauge on the top had a significant effect. The hydrostatic pressure for a 10 μm depth of saturated mixture is 17 mPa and for pure ^3He 11 mPa, so we could easily observe changes in the crystal position, and even the movement of the phase boundary, at 10 μm

level. Another factor with a potential contribution to the measured data is the pressure arising from the surface tension and curvature of the ^4He crystal. This effect is strongest at the limit of a very small crystal, but has an observable contribution if the curvature of the crystal is less than 2.5 mm as estimated in publication X.

The performance of the gauge with regard to resolution and sensitivity was satisfactory, but the heating caused by operation had unacceptable levels. When the gauge was installed directly into the experimental volume of the adiabatic melting experiment, the measured increase in heatleak to the liquid was 100 pW at excitation levels that permitted capacitance readings at the full precision of the bridge (about 1 V). It seems that the heating is unavoidable if the capacitance, and thus the pressure, is to be measured at the desired precision. So the pressure gauge was detached thermally and mechanically from the cell and anchored separately to the nuclear state. The detached pressure gauge has been tested at millikelvin temperatures and proven to have the same performance as in the original setup. In the next try of the adiabatic melting, the pressure of the main volume will be relayed to the detached pressure gauge via a small and long capillary, in order to eliminate conducted heat.

Chapter 3

Studies on properties of helium mixtures

The detached pressure gauge with the superleak filling lines, shown in figure 3.1 **III**, was a suitable setup for measurements on the properties of helium mixtures at a pressure and temperature range not investigated before. The superleak line allowed raising the pressure of the studied mixture, by inserting ^4He to the sample volume, well above the melting pressure of pure ^4He [18], all the way up to the melting pressure of ^4He in saturated mixture. The sensitive pressure transducer and a quartz tuning fork resonator were at disposal for accurate analysis on the sample properties.

We measured the osmotic pressure of helium mixture at the melting pressure for various concentrations, and the maximum solubility of ^3He in the dilute phase from zero pressure to the melting pressure. As the carefully prepared adiabatic melting experiment operates at the melting pressure of the mixture, knowing these properties is crucial. The measured data can also be used to determine the effective mass, and the effective two-particle interaction potential for the quasi-particles in a dilute mixture. When these are known, almost any thermodynamic property of the mixture can be calculated at any given pressure.

Both series of measurements were done in a single cooldown lasting several months. The concentration of the sample was increased, starting from pure ^4He up to almost 10% of ^3He in 33 nearly equal steps. The stepwise increase of the ^3He content without a need to warm the cell to kelvin temperatures was possible because the superleak line could be used as a filter for ^3He . The new dose of ^3He was prepared at room temperature and pushed into the cell through a normal capillary by large flow of ^4He . The pressure of the cell could be kept constant

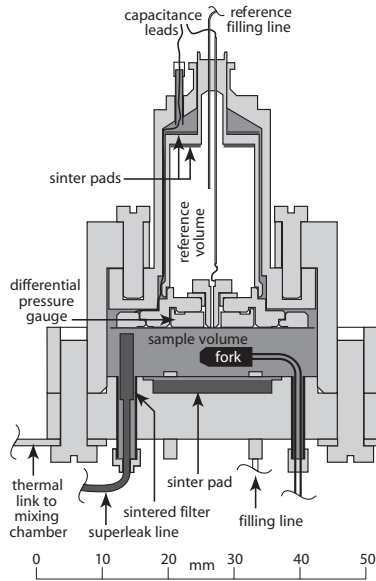


Fig. 3.1 Cross section of the detached pressure gauge used as experimental cell in osmotic pressure and solubility measurements. The capacity of the sample volume was $8.3 \pm 0.2 \text{ cm}^3$ and that of the reference volume 18 cm^3 .

as ^4He could be extracted through the superleak while the ^3He dose was being flushed in. New doses were added at approximately 0.1 MPa pressure and at about 10 mK temperature.

3.1 Solubility of ^3He in ^4He at millikelvin temperatures

We measured the low-temperature solubility of ^3He in the dilute phase for the whole pressure range where dilute mixtures exist. During the measurements, the amount of inserted ^3He was followed by careful bookkeeping. Determining the concentration of the sample based on this alone is not sufficiently accurate, since thermal gradients in the filling lines and heat exchange sinters cause unknown concentration gradients. Therefore, we observed the change of the sample den-

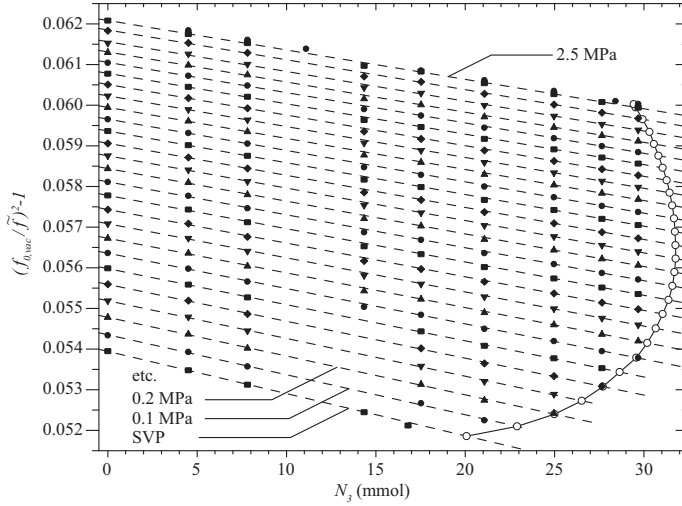


Fig. 3.2 The density of the $^3\text{He}/^4\text{He}$ mixture indicated as a change in the idealized resonance frequency \tilde{f} of the tuning fork as a function of the added ^3He for selected pressures. The open symbols show the response in saturated mixture, the closed symbols for homogenous mixtures, and the dashed lines are fits to each pressure.

sity directly with the quartz tuning fork immersed in the sample volume. For an ideal inviscid hydrodynamic liquid, the inverse square of the fork's resonance frequency f_0 is linearly dependent on the density of the medium

$$\left(\frac{f_{0,vac}}{f_0}\right)^2 = 1 + B \frac{\rho_{liq}}{\rho_{body}}, \quad (3.1)$$

where $f_{0,vac}$ is the resonance frequency in vacuum, ρ_{liq} and ρ_{body} are the densities of the liquid and the resonator body, and B is a numerical factor of order of unity **III**. A helium mixture at the studied temperature range is far from an ideal liquid and the viscosity has a strong effect on the the resonance frequency. This effect can be taken into account by examining a weighted sum of the frequency f_0 and width w of the resonance $\tilde{f} = f_0 + w/4$, which is found to approximate the inviscid limit in measurements with forks **III** as well as with vibrating wire resonators [33].

The fork response at 10 mK temperature and at about 0.1 MPa pressure was measured for each amount of added ^3He . The cell was pressurized up to the melting pressure at constant 10 mK temperature for ten equally spaced ^3He densities,

while the fork response was continuously measured. The pressure of the cell was controlled by the amount of pure ^4He , so for a certain amount of inserted ^3He , the ^3He partial density was constant, but the concentration depended on pressure. For a selected pressure, according to equation 3.1, the inverse squares of the idealized frequencies \tilde{f} for different ^3He densities should lie on a straight line, as can be seen in figure 3.2 **III**. The presence of pure ^3He phase causes the fork response to saturate to a constant value set by the saturation concentration of the mixture at the examined pressure.

We were able to determine the relative saturation concentration over the pressure range from zero to the melting pressure with ± 0.003 precision. To get absolute concentrations some uncertain quantities, namely the volume of the cell and the bookkeeping of inserted helium must be used, and accuracy decreases. If the noted values are used, the saturation concentration at zero pressure is 6.8%, at the maximum of solubility at about 1 MPa it is 9.7%, and at the melting curve it is 8.3%. These values coincide reasonably well with literature values. For a more complete review see, publication **III**.

3.2 Osmotic pressure of $^3\text{He}/^4\text{He}$ mixtures

If a system consisting of several distinguishable components is separated to closed volumes so that chemical potential of one of the components is linked over the separating boundary, a concentration difference over the boundary generates a pressure difference in thermal equilibrium. This pressure difference is called osmotic pressure π and it is a useful concept in understanding the system, since it is a macroscopically measurable quantity, but depends on the microscopic thermodynamical description.

Usually osmotic pressure in helium liquids is studied in a divided cell where the two parts are connected with a piece of superleak to allow flow of ^4He between the volumes to equalize the chemical potentials. In our measurement, we studied the osmotic pressure at the melting pressure of the mixture. Pure ^4He solids in both volumes were used to relate the thermodynamic properties of the two sides. Also, instead of the osmotic pressure, the actual measured quantity was the difference in the crystallization pressures of pure ^4He and the studied mixture Δp^c . These two pressure differences are related by a simple linear relationship

$$\pi = 0.095 \cdot \Delta p^c. \quad (3.2)$$

derived in publication **I**.

For ten ^3He densities, the sample was pressurized to the melting pressure and the melting curve was measured over a temperature range from about 5 mK to 60 mK. The melting pressures at discrete temperatures were measured with the sensitive differential pressure gauge, using partially solid pure ^4He as reference. The pressure of the cell was raised by inserting ^4He through the superleak. For a pressure, exceeding the melting pressure, the eventual nucleation of the solid phase was seen as a rapid drop in the pressure as the overpressure required for the nucleation relaxed. After nucleation, the solid phase was grown incrementally to allow extrapolating the melting pressure to zero limit of the solid size as explained in publication I.

Below the Fermi temperature, entropy of the dilute phase is directly proportional to T and the osmotic pressure has a quadratic temperature dependence, as can be seen from equations 2.2 and 3.2. Fits to the low-temperature part of experimental data were used to extract the osmotic pressures at the zero temperature limit, and the coefficient of the quadratic temperature dependence. The results of the fits along with theoretical curves [5] are shown in figure 3.3 I. The fits give the zero temperature limit quite precisely while the slopes have considerable statistical scatter.

The theoretical curve is a result of a numerical calculation. The effective two particle interaction potential significantly influences the zero temperature limit of the osmotic pressures, while the effective mass m^* has a strong effect on the steepness of the quadratic temperature dependence. Neither of these factors have previously been measured at pressures this high and so the measured data were used to get estimates for these.

The effective mass could be estimated by considering the system as a noninteracting fermi system and iteratively adjusting m^* so that the theoretical curve coincided with the measurements. The estimate for the effective mass at the melting pressure was $m^* = 2.91m_3$, where m_3 is the mass of a ^3He atom, which is well in line with literature values at lower pressures. The fitting procedure for the ^3He - ^3He effective interaction potential was rather more complicated. Data from the solubility measurements were used along with the osmotic pressure measurements, and the potential was determined for the whole pressure range from zero to the melting pressure. The potential is discussed briefly in publication I, and a more comprehensive article on the subject is in preparation [5]. To give some perspective, the potential has the strongest contribution to the quasi-particle energy at saturation concentration and zero pressure, when its magnitude is about 30% of the Fermi energy.

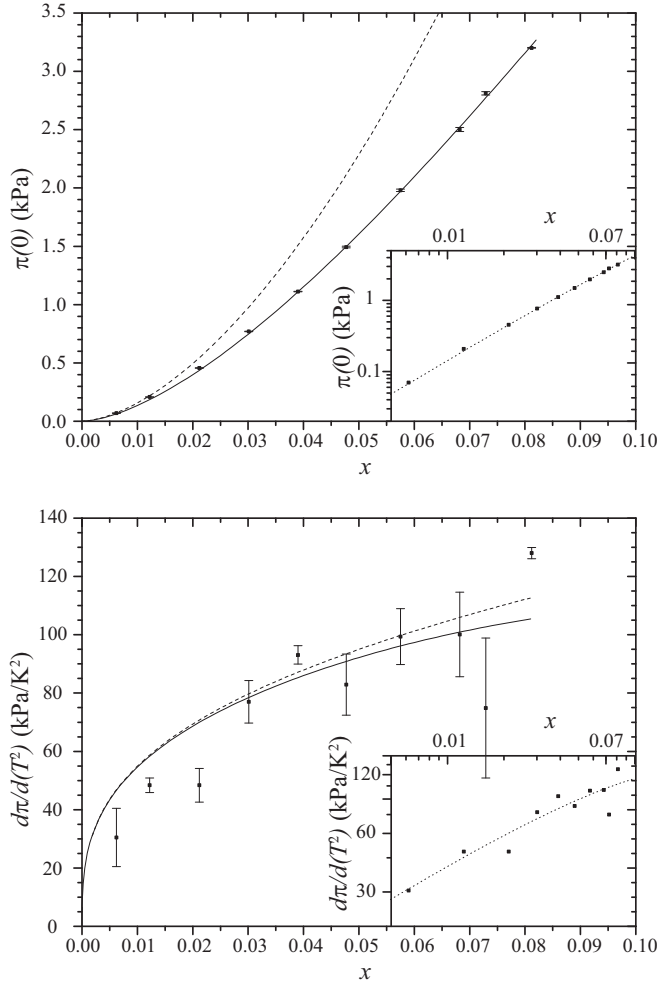


Fig. 3.3 Osmotic pressure at zero temperature (top) and coefficient of quadratic temperature dependence (bottom) as a function of concentration. The symbols with error bars are the measured values, the solid lines are results of a theoretical calculation using a fitted interaction potential for the quasiparticles, and the dashed lines are results when the interactions are omitted. The insets show the same data on logarithmic scales along with semiempirical fits.

Chapter 4

Conclusions

In our experiment with the adiabatic melting for cooling helium mixtures, the method was proven to be highly potential but challenging. The method acts directly on the liquid, so it could possibly circumvent the so called Kapitza barrier, at about 100 μK temperature, caused by the rapidly increasing thermal resistance between any external refrigerant and the fluid. Definite cooling was observed when melting of the ^4He solid was initiated, but technical shortcomings of the experimental setup prevented reaching temperatures close enough to the theoretically predicted limit. The reasons for the limited performance are known, the main shortcomings being a smaller than desired cooling power caused by mass flow problems with the superleak lines, and the non-adiabaticity caused by heatleaks from the cell structures and thermometry. The problems are not trivial: even five years after the first test, the improved setup is not ready for another try. Still, if the study of helium mixtures and the search for superfluidity of dilute mixture is desired to be continued, the adiabatic melting method seems to give the most plausible mean to cool the fluid below 100 μK temperature.

We also studied the problems concerning thermometry of the helium mixture. The same thermal resistance barrier that hinders external refrigeration of helium liquids also complicates the thermometry by preventing thermalization of any external thermometer with the helium mixture. The adiabatic melting method uses the properties of helium to produce cooling, and correspondingly, also the thermometry must be based on some directly measurable temperature-dependent property of the helium mixture itself. We have used the melting pressure of the solid ^4He in the mixture and the dissipation imposed by the helium mixture or the pure ^3He phase of a phase-separated mixture on mechanical resonators as a basis for thermometry.

Melting pressure thermometry for pure ^3He is a well established method in low-temperature experiments. Instead of pure ^3He , our sample consisted of a helium mixture that, upon pressurizing at a temperature below 50 mK, forms an univariant system of solid ^4He , liquid dilute helium mixture at saturation concentration, and liquid pure ^3He . The melting pressure was measured by a differential capacitive pressure gauge using ^4He melting pressure as reference. The performance of the gauge was good, the resolution at the melting pressure was 0.01 Pa. This would allow thermometry to temperatures below 100 μK , when the deviation of the melting curve from quadratic behavior at temperatures approaching T_c of the pure ^3He phase is properly taken into account.

Mechanical resonators are also well established tools for probing quantum fluids. We have used vibrating wire resonators and quartz tuning forks to observe the temperature, concentration, and pressure of helium fluids. In the first run with the complete adiabatic melting setup, two vibrating wires were installed, one positioned in the saturated mixture (lower) and one in the pure ^3He phase (upper). The upper wire was used as thermometer by measuring the exponentially decaying dissipation by the superfluid on the moving wire. The performance was rather limited due to the intrinsic losses inflicted by the complicated structures for supporting the wire and generating the magnetic field. The temperature sensitivity saturated already at about 300 μK temperature. The lower wire was designed to detect the possible superfluid transition of the dilute phase.

We also studied quartz tuning forks as possible replacements for vibrating wires. Tuning forks were found to be superior in many aspects. Their intrinsic damping is very small, which permits higher sensitivity for detecting the dissipation by the medium. The density of quartz is smaller than that of metallic wires, which enhances the sensitivity for dispersion by the medium. The higher resonance frequency decreases the viscous penetration depth, which increases the Q-value when the fork is used in highly viscous medium, making it easier to resolve the resonance characteristics. Forks are also rather easy to measure, do not need magnetic field for operation nor are they affected by one, and can be acquired cheaply and in large quantities from electronics suppliers. Their drawbacks, compared to vibrating wires, are a more complex geometry, which makes analysis more difficult, larger size, and in some aspects also the higher resonance frequency, which can lead to acoustic losses that will also complicate the data analysis.

The acoustic modes, strongly coupled to the forks in helium fluids at suitable conditions, are a bare nuisance in most situations. To escape these, the resonance condition should be avoided by selecting the fork and the experimental cavity dimensions so that standing waves can not be excited in the medium de-

sired to be studied. We also contemplated on using the acoustic modes as fixed points in thermometry. The modes are extremely sharp, and thus provide good resolution. On the other hand, the complex geometry prevents determining exactly when and where these modes occur. In our measurements, we have shown that single modes in a complex pattern can be identified and followed. The general characteristics of the resonance pattern for a fork in a cylindrical cavity has also been reproduced in numerical simulations [34].

Besides the more technical studies related to cooling and thermometric methods, we also measured some properties of helium mixtures in conditions not surveyed before. The solubility of ^3He in ^4He was measured over the whole pressure range from zero up to the melting pressure. At the melting pressure, the osmotic pressure was measured at several concentrations. Based on these measurements, the effective interaction potential between ^3He quasiparticles was deduced over a wide pressure and concentration range. The interaction potential can be used to calculate basically any thermodynamic property of the mixture. For the superfluid transition close to the melting pressure, this potential prefers p-wave pairing and gives $T_c \approx 40 \mu\text{K}$ [5].

Even though studying helium mixtures at ultra low temperatures is experimentally an extremely difficult task, and obtaining valid results is tedious and even uncertain, it still offers such a diverse model system for quantum mechanical phenomena that these pursuits deserve to be continued.

References

- [1] F. Pobell, *Matter and Methods at Low Temperatures* (Springer-Verlag, 1992).
- [2] A. Griffin, *J. Phys. Condens. Matter* **21**, 164220 (2009).
- [3] D. D. Osheroff, R. C. Richardson, and D. M. Lee, *Phys. Rev. Lett.* **28**, 885 (1972).
- [4] J. Bardeen, G. Baym, and D. Pines, *Phys. Rev.* **156**, 207 (1967).
- [5] J. Rysti, J. Tuoriniemi, and A. Salmela, *Phys. Rev. B* **Submitted** (2012).
- [6] J. Tuoriniemi, J. Martikainen, E. Pentti, A. Sebedash, S. Boldarev, and G. Pickett, *J. Low Temp. Phys.* **129**, 531 (2002).
- [7] A. M. Guénault, V. Keith, C. J. Kennedy, and G. R. Pickett, *Phys. Rev. Lett.* **50**, 522 (1983).
- [8] H. Ishimoto, H. Fukuyama, N. Nishida, Y. Miura, Y. Takano, T. Fukuda, T. Tazaki, and S. Ogawa, *J. Low Temp. Phys.* **77**, 133 (1989).
- [9] G. Oh, Y. Ishimoto, T. Kawae, M. Nakagawa, O. Ishikawa, T. Hata, T. Kodama, and S. Ikehata, *J. Low Temp. Phys.* **95**, 525 (1994).
- [10] A. Sebedash, *JETP Lett.* **65**, 276 (1997).
- [11] A. P. Sebedash, *Physica B* **284-288**, 325 (2000).
- [12] R. L. Rusby, M. Durieux, A. L. Reesnik, R. P. Hudson, G. Schuster, M. Kuhne, W. E. Fogle, R. J. Soulen, and E. D. Adams, *J. Low Temp. Phys.* **126**, 633 (2002).
- [13] J. T. Tough, W. D. McCormick, and J. G. Dash, *Phys. Rev.* **132**, 2373 (1963).

- [14] D. O. Clubb, O. V. L. Buu, R. M. Bowley, R. Nyman, and J. R. Owers-Bradley, *J. Low Temp. Phys.* **136**, 1 (2004).
- [15] R. Blaauwgeers, M. Blazkova, M. Človečko, V. B. Eltsov, R. de Graaf, J. Hosio, M. Krusius, D. Schmoranzer, W. Schoepe, L. Skrbek, P. Skyba, R. E. Solntsev, and D. E. Zmeev, *J. Low Temp. Phys.* **146**, 537 (2007).
- [16] H. Preston-Thomas, *Metrologia* **27**, 3 (1990).
- [17] W. Yao, T. A. Knuutila, K. K. Nummila, J. E. Martikainen, A. S. Oja, and O. V. Lounasmaa, *J. Low Temp. Phys.* **120**, 121 (2000).
- [18] E. Smith, D. Brewer, C. Liezhao, and J. Reppy, *Physica B+C* **107**, 585 (1981).
- [19] D. O. Edwards and S. Balibar, *Phys. Rev. B* **39**, 4083 (1989).
- [20] D. Bradley, S. Fisher, A. Guénault, R. Haley, M. Holmes, S. O'Sullivan, G. Pickett, and V. Tsepelin, *J. Low Temp. Phys.* **150**, 364 (2008).
- [21] J. Jäger, B. Schuderer, and W. Schoepe, *Phys. Rev. Lett.* **74**, 566 (1995).
- [22] G. G. Stokes, *Mathematical and Physical Papers*, Vol. 3 (Cambridge University Press, London, 1901).
- [23] T. H. Virtanen and E. Thuneberg, *Phys. Rev. Lett.* **106**, 055301 (2011).
- [24] T. H. Virtanen and E. V. Thuneberg, *Phys. Rev. B* **83**, 224521 (2011).
- [25] D. C. Carless, H. E. Hall, and J. R. Hook, *J. Low Temp. Phys.* **50**, 583 (1983).
- [26] H. Højgaard Jensen, H. Smith, P. Wölfle, K. Nagai, and T. Maack Bisgaard, *J. Low Temp. Phys.* **41**, 473 (1980).
- [27] R. M. Bowley and J. R. Owers-Bradley, *J. Low Temp. Phys.* **136**, 15 (2004).
- [28] A. M. Guénault, V. Keith, C. J. Kennedy, and G. R. Pickett, *Phys. Rev. Lett.* **50**, 522 (1983).
- [29] S. Perisanu and G. Vermeulen, *Phys. Rev. B* **73**, 134517 (2006).
- [30] J. Martikainen, J. Tuoriniemi, T. Knuutila, and G. Pickett, *J. Low Temp. Phys.* **126**, 139 (2002).
- [31] D. C. Carless, H. E. Hall, and J. R. Hook, *J. Low Temp. Phys.* **50**, 605 (1983).

-
- [32] A. M. Guénault, V. Keith, C. J. Kennedy, S. G. Mussett, and G. R. Pickett, *J. Low Temp. Phys.* **62**, 511 (1986).
- [33] J. Martikainen, J. Tuoriniemi, T. Knuuttila, and G. Pickett, *J. Low Temp. Phys.* **126**, 139 (2002).
- [34] J. Tuoriniemi, J. Rysti, A. Salmela, and M. Manninen, *J. Phys. Conf. Ser.* **Accepted** (2012).



ISBN 978-952-60-4582-5
ISBN 978-952-60-4583-2 (pdf)
ISSN-L 1799-4934
ISSN 1799-4934
ISSN 1799-4942 (pdf)

Aalto University
Aalto University School of Science
O.V. Lounasmaa Laboratory
www.aalto.fi

**BUSINESS +
ECONOMY**

**ART +
DESIGN +
ARCHITECTURE**

**SCIENCE +
TECHNOLOGY**

CROSSOVER

**DOCTORAL
DISSERTATIONS**